Dentomaxillofacial Radiology (2015) 44, 20150011

birpublications.org/dmfr

RESEARCH ARTICLE

3-T MRI safety assessments of magnetic dental attachments and castable magnetic alloys

[1]M Hasegawa, [1]K Miyata, [1]Y Abe, [1]T Ishii, [1,2]T Ishigami, [1,2]K Ohtani, [1,2]E Nagai, [1,2]T Ohyama, [1,2]Y Umekawa and [1,2]S Nakabayashi

[1]Department of Partial Denture Prosthodontics, Nihon University School of Dentistry, Tokyo, Japan; [2]Division of Clinical Research, Nihon University School of Dentistry, Tokyo, Japan

Objectives: To assess the safety of different magnetic dental attachments during 3-T MRI according to the American Society for Testing and Materials F2182-09 and F2052-06e1 standard testing methods and to develop a method to determine MRI compatibility by measuring magnetically induced torque.
Methods: The temperature elevations, magnetically induced forces and torques of a ferromagnetic stainless steel keeper, a coping comprising a keeper and a cast magnetic alloy coping were measured on MRI systems.
Results: The coping comprising a keeper demonstrated the maximum temperature increase (1.42 °C) for the whole-body-averaged specific absorption rate and was calculated as 2.1 W kg^{-1} with the saline phantom. All deflection angles exceeded 45°. The cast magnetic alloy coping had the greatest deflection force (0.33 N) during 3-T MRI and torque (1.015 mN m) during 0.3-T MRI.
Conclusions: The tested devices showed minimal radiofrequency (RF)-induced heating in a 3-T MR environment, but the cast magnetic alloy coping showed a magnetically induced deflection force and torque approximately eight times that of the keepers. For safety, magnetic dental attachments should be inspected before and after MRI and large prostheses containing cast magnetic alloy should be removed. Although magnetic dental attachments may pose no great risk of RF-induced heating or magnetically induced torque during 3-T MRI, their magnetically induced deflection forces tended to exceed acceptable limits. Therefore, the inspection of such devices before and after MRI is important for patient safety. *Dentomaxillofacial Radiology* (2015) **44**, 20150011. doi: 10.1259/dmfr.20150011

Cite this article as: Hasegawa M, Miyata K, Abe Y, Ishii T, Ishigami T, Ohtani K, et al. 3-T MRI safety assessments of magnetic dental attachments and castable magnetic alloys. *Dentomaxillofac Radiol* 2015; **44**: 20150011.

Keywords: magnetic resonance imaging; temperature; equipment safety; magnetic phenomena; dental prosthesis

Introduction

MRI is a technique that displays the body in thin tomographic slices. However, radiofrequency (RF) heating of metallic medical implants in patients during MRI has always been a safety concern; it has received greater attention because of the increased application of interventional MRI and frequent use of a large number of RF pulses to achieve a short scan duration.[1–9] Another consideration is that translational attraction and torque from magnetic field interactions may cause the movement or dislodgment of a ferromagnetic implant, resulting in an uncomfortable sensation or injury to the patient. Translational attraction is dependent on the

Correspondence to: Dr Mikage Hasegawa. E-mail: mikagehasegawa@gmail.com
This study was supported by JSPS KAKENHI 26462940, Dental Research Center, Nihon University School of Dentistry, and a grant from the Dental Research Center, Nihon University School of Dentistry to Yuki Abe; and by Mikage Hasegawa, Kazuyuki Miyata and Yuki Abe.
Received 10 January 2015; revised 5 March 2015; accepted 17 March 2015

strength of the static magnetic field, the spatial gradient magnetic field and the object's mass, shape and magnetic susceptibility. The effects of translational attraction on external and implanted ferromagnetic objects are predominantly responsible for possible hazards in the immediate vicinity of the MR system.[10–12]

Magnetic dental attachments are now commercially available for use in dental treatments. Many improvements, especially in corrosion prevention, increasing the attractive force, and size reduction have been introduced, thus contributing to the popularity of magnetic attachments.[13] Such attachments are excellent retainers for removable partial dentures because they reduce trauma to the supporting teeth and dissipate the lateral stress component to the abutment teeth, thus improving prosthesis retention and maintaining a semi-permanent retentive force. They are useful not only in prosthodontics but also in maxillofacial prosthetics.[14–16] Most commercially available magnetic attachments consist of two small components: a keeper, which is generally composed of stainless steel, and its corresponding magnetic assembly.[8,17] A problem associated with the common usage of magnetically attached dentures is the presence of a small non-removable ferromagnetic keeper in the oral area. However, to improve the strength of the denture base and to reduce trauma to the supporting teeth, castable magnetic alloy is occasionally used instead of a keeper because it can be cast into various shapes, thus improving the flexibility of denture design.[17] Therefore, one must be aware of the possible presence of a large amount of magnetic alloy in the oral area.

The American Society for Testing and Materials (ASTM) requires a determination of whether the presence of a passive implant could cause injury to an implanted individual during an MRI procedure.[9,10,18] ASTM testing methods cover RF-induced heating, deflection force and torque.

The safety of magnetic dental attachments has been reported according to the ASTM F2182-02a standard test method for RF-induced heating.[17,19] Since then, the method has been considerably revised;[9] the changes include different measurement conditions, such as the implant location within the phantom, the composition of the phantom and the procedure to determine the specific absorption rate (SAR) calorimetrically. For a proper evaluation of safety, research according to the revised standard is required. Moreover, there are some difficulties in adapting the ASTM F2213 standard to magnetically induced torque in the ferromagnetic material of keepers.

We aimed to investigate the MRI compatibility and safety of magnetic dental attachments, including castable magnetic alloys, during 3-T MRI according to the ASTM F2182-09 and F2052-06e1 standard testing methods, and to produce a measurement method to evaluate the potential hazards of magnetically induced torque.

Methods and materials

Assessment of radiofrequency-induced heating

MRI system: Measurements were performed on a 3-T MRI scanner (MAGNETOM® Verio with Syngo® MR B17 software; Siemens Healthcare, Erlangen, Germany).

Dental devices: Three types of magnetic dental devices were tested in this study; a keeper made of ferromagnetic stainless steel (GIGAUSS D600; GC, Tokyo, Japan), a coping (Coping A) comprising a keeper and cast alloy (Pallatop 12 Multi; Dentsply-Sankin, Tochigi, Japan) and a coping (Coping B) composed of cast magnetic alloy (Attract P; Tokuriki-Honten Co., Ltd, Saitama, Japan) (Table 1). The keeper of Coping A was cemented with standard luting cement (Fuji Luting Cement; Shofu, Kyoto, Japan). Coping A and Coping B were almost the same in form.

Measurement points: The measurement points on the dental devices are shown in Figure 1. On the basis of the results of a pilot experiment, Fluoroptic® thermometry probes (0.5-mm diameter, Model MedFP™; LumaSense Technologies, Inc., Santa Clara, CA) were positioned at locations showing the greatest heating during MRI: Probe 1 was placed in contact with the side of the keeper or upper surface of the coping; Probe 2 was placed in contact with marginal gingival tissue adjacent to the coping; and Probe 3 was placed in contact with the apex of the coping post. Each device was positioned on acrylic resin posts 2 cm from the surface and at the centre of the left-side walls of the phantoms. The longest

Table 1. Dental devices tested in the study

Device	*Material*	*Composition (% mass)*	*Dimensions (mm)*	*Mass (g)*
Keeper	GIGAUSS D400 (GC, Tokyo, Japan)	UNS S44627	$\phi 3.0 \times 0.6$	0.034
	GIGAUSS D600 (GC)	UNS S44627	$\phi 3.6 \times 0.7$	0.058
	GIGAUSS D1000 (GC)	UNS S44627	$\phi 4.9 \times 0.8$	0.119
Coping A	GIGAUSS D600 (GC)	UNS S44627	$\phi 3.6 \times 0.7$	0.058
	Pallatop 12 Multi (Dentsply-Sankin, Tochigi, Japan)	12% Au, 20% Pd, 50% Ag, 15% Cu, 3% other	10 (length)	0.941
Coping B	Attract P (Tokuriki-Honten Co., Ltd, Saitama, Japan)	3% Au, 14% Ag, 48% Pd, 32% Co, 3% other	10 (length)	0.927

Ag, silver; Au, gold; Co, cobalt; Cu, copper; Pd, palladium; UNS, unified numbering system.

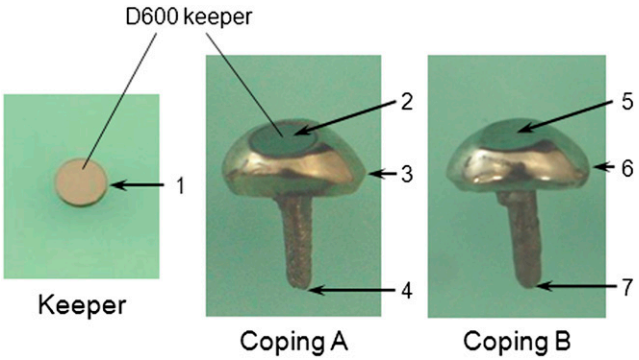

Figure 1 Measurement points on the tested devices for the radiofrequency-induced heating test. Point 1 is on the side of the keeper; Points 2 and 5, the upper surfaces of the copings; Points 3 and 6, marginal gingival tissue adjacent to the coping; and Points 4 and 7, the apex of the coping post.

linear dimension of the devices was aligned with the static magnetic field. Probe 4 was used as the reference probe and placed on the right sides of the phantoms with its longitudinal axis passing through the geometric centre of the phantoms as the reflection axis.

Saline and tissue-equivalent phantoms and temperature measurements: According to the revised ASTM standard test method,[17] the whole-body-averaged SAR was calculated in a saline phantom of 65 cm (length) × 42 cm (width) × 9 cm (depth) to determine the maximum RF irradiation parameters before the heating test. Temperature measurements were also performed in a tissue-equivalent phantom that conformed to the revised ASTM phantom model specification.[17] Temperature elevation after RF irradiation was measured by using a Fluoroptic® thermometry system (model 3300; LumaSense™ Technologies, Inc.) and probes; details of its design and procedure have been described previously.[20]

Assessment of magnetically induced deflection forces

MRI system: Measurements were performed on a 3-T MRI scanner (MAGNETOM Verio with Syngo MR B17 software).

Dental devices: Five types of magnetic dental devices were tested in this study (Table 1): three keepers made of ferromagnetic stainless steel (GIGAUSS D400, D600 and D1000; GC), a coping (Coping A) comprising a keeper and cast alloy (Pallatop 12 Multi) and a coping (Coping B) composed of cast magnetic alloy (Attract P). The keeper of Coping A was cemented with standard luting cement (Fuji Luting Cement).

Deflection force measurements: Deflection force was assessed by using the deflection angle method described in the relevant ASTM standard testing method.[18] When the deflection angle exceeded 45°, loads were added to determine the weight required to constrain the deflection angle within 45°. In addition, for a deflection angle ≥65°, additional measurements were performed with non-ferromagnetic weights attached to the thread to improve the accuracy of the force measurement.[21,22] Details of the design and procedure have been described previously.[20]

Assessment of magnetically induced torque forces

MRI system: Measurements were performed on a 0.3-T MRI scanner (AIRIS Vento; Hitachi Medical Corporation, Tokyo, Japan).

Dental devices: The same five types of magnetic dental devices tested in the deflection force experiments were tested in this study (Table 1).

Apparatus: A torque angle indicator was produced from a non-ferromagnetic material unaffected by magnetic forces (Figure 2). The torque angle indicator consists of a sturdy structure supporting a holding platform, torsional spring, torsional spring control knob, protractor and torque driver connector. The torsional spring strength is changeable with a torsional spring knob according to the torque strength of the test device.

The torque angle is output numerically when the angle is reproduced by a Micro Torque Driver (Tohnichi Mfg. Co., Ltd, Tokyo, Japan) with a torque driver connector (Figure 2).

Torque measurement procedure: The testing device was attached to the holding platform, and the platform was rotated by torque at the centre of the magnetic field. The supporting structure was fixed to a protractor with a 1° graduated marker to measure the angle between the platform and the supporting structure. Measurements

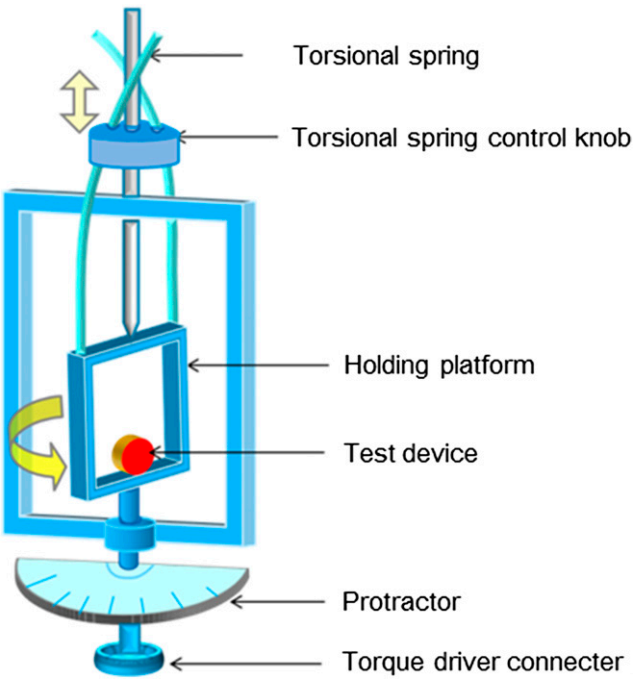

Figure 2 Diagram of the torque angle indicator.

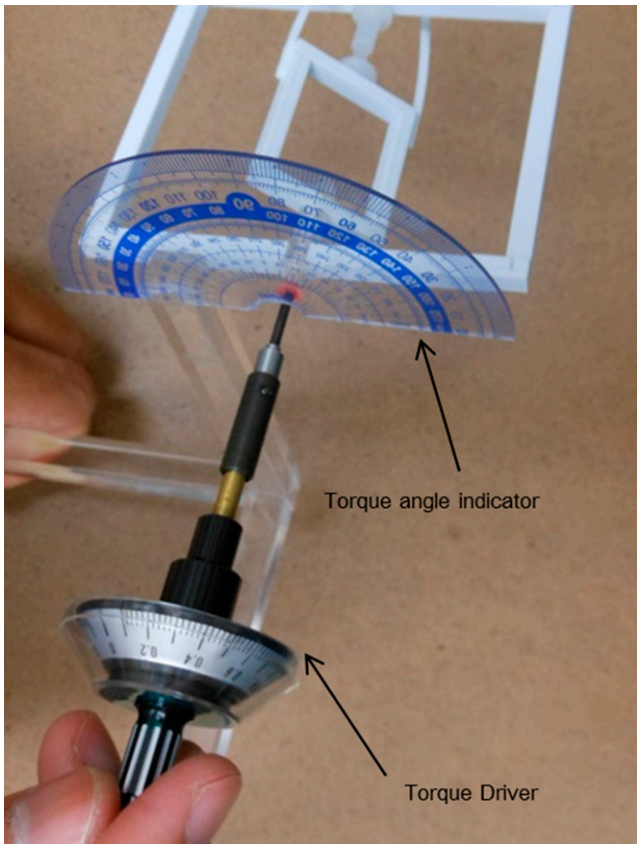

Figure 3 The torque driver and torque angle indicator.

were performed three times for each of the three axial directions (*x*-, *y*- and *z*-axis), and the maximum angles were determined. Outside the MRI room, the Micro Torque Driver was attached to the connector and rotated to the angle measured by the test devices; therefore, the torque angle is reported numerically (Figure 3). To confirm the accuracy of the torque angle indicator, we compared the calculated torques from a tubular spring scale (D95156; Sanko Seikohjyo Co. Ltd, Tokyo, Japan), which demonstrated an accuracy of 1.0 g compared with torque measurements from the Micro Torque Driver.

Results

Radiofrequency-induced heating

The previously reported[20] and new data from the tested devices according to the ASTM 2182-02a standard testing method are presented in Table 2. The maximum temperature increases were 1.21 °C for the keepers, 1.42 °C for Coping A and 1.30 °C for Coping B (Table 3). The calorimetrically measured whole-body SAR was 2.1 W kg^{-1}.

Deflection force

All devices were strongly attracted to the MRI system, and their deflection angles exceeded 90°. The keepers required an additional 5-g load to constrain their deflection angles within 45°; Copings A and B required loads of 4 and 34 g, respectively (Figure 4a). The magnetically induced deflection forces of the devices are reported in Figure 4b. Coping B demonstrated the greatest deflection force.

Table 2 Reported and additional data from radiofrequency-induced heating tests conducted according to the American Society for Testing and Materials F2182-02a method

Device	*Maximum temperature increase (°C)*
Phantom contents	+0.2
Keeper	+0.3
Coping A	+0.6
Coping B	+0.6

The result for Coping A was reported previously.[20]
The MR system used was an Achieva 3.0 T Nova Dual (Philips, Tokyo, Japan).

Deflection torque

The magnetically induced torques of the devices are shown in Figure 5. Coping B demonstrated the greatest deflection torque. The force of the torque increases with the keeper volume.

Discussion

The SAR is an important factor indicating the safety level from RF-induced heating.[3] However, the console-reported SARs across MR systems show low correlations because of different SAR calculation methods.[23,24] In the present study, the revised ASTM standard test method (ASTM F2182-09) was applied to measure temperature elevation in a saline phantom.

Temperature elevation is affected by measurement conditions such as the volume and composition of the phantom material and locations of the specimens in the phantom.[3,21,22] Therefore, the testing methods were defined more specifically in the ASTM F2182-09 standard, such as device location, the method of phantom preparation and design of the implant holder. Furthermore, with this testing method, the terms provide comparative values of RF power and time. Because sequence parameter correlations among MRI systems are low, evaluating the RF-induced heating caused by each sequence would not be meaningful. However, the results of an experiment conducted according to a standard testing method are applicable to other MR sequences to estimate RF-induced heating levels from the SAR.

In a previous study,[17] the phantom volume was 4 l, and the specimens were located at the centre of the phantom. In this study, the phantom volume was 25 l and the specimens were located 2 cm from the phantom wall to ensure the most severe heating conditions. However, the tested devices showed minor temperature elevations in both studies. The heat–pain threshold of the oral mucosa has already been studied.[25–27] A

Table 3 Temperature elevation of the devices at each measurement point

Device	*Maximum temperature increase (°C)*
Keeper	
Point 1	+1.21
Without the prosthesis	+1.13
Coping A	
Point 2	+1.42
Point 3	+1.36
Point 4	+1.36
Without the prosthesis	+1.13
Coping B	
Point 5	+1.30
Point 6	+1.24
Point 7	+1.19
Without the prosthesis	+1.13

Point 1 is located at the side of the keeper; Points 2 and 5, the upper surfaces of the copings; Points 3 and 6, marginal gingival tissue adjacent to the coping; and Points 4 and 7, the apices of the coping posts.

temperature rise of approximately 8–10 °C causes pain in the oral mucosa. An elevation of 10 °C above the body temperature for 1 min constitutes the safety threshold for periodontal tissue, which is less susceptible to thermal injury than the bone because of its greater vascularity.[17,28,29] In the present study, Coping A showed the maximum temperature elevation, but it was only 1.42 °C during a whole-body SAR of 2.1 W kg^{-1} calculated from the saline phantom. This temperature increase would be insufficient to affect periodontal tissue or cause pain. Therefore, none of the tested devices should pose a risk to patients during 3-T MRI.

Another MRI safety concern with metallic devices is magnetically induced deflection forces and torques that may cause the migration of such devices and injure the patient.[11,30]

According to the relevant ASTM F2052-06 standard for magnetically induced displacement force,[10] if the device deflects <45°, the risk imposed by the magnetically induced deflection force would be no greater than that imposed by normal daily activity in the Earth's gravitational field. In this study, all devices were strongly attracted to the MR system, and their deflection angles were >90°. Therefore, magnetic attachments may cause discomfort to the patient during MRI. The calculated deflection forces of Copings A and B were approximately 0.03956 N (3956 dyn) and 0.33205 N (33204.8 dyn), respectively. However, the retention force of the dental luting cement between the keeper and coping is reportedly 48–150 N,[31] which is sufficiently strong. Nevertheless, the fixation of ferromagnetic

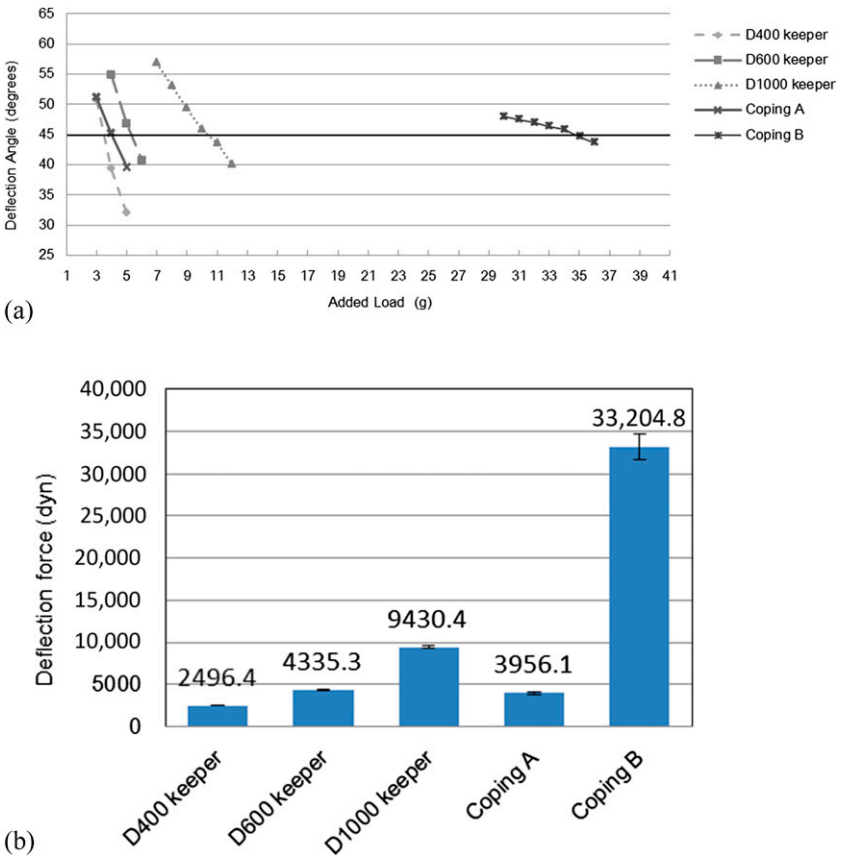

Figure 4 (a) Deflection angles observed for the tested devices with added loads. (b) The mean magnetically induced deflection forces of the tested devices (1 dyn = 10^{-5} N). Bars indicate standard deviations.

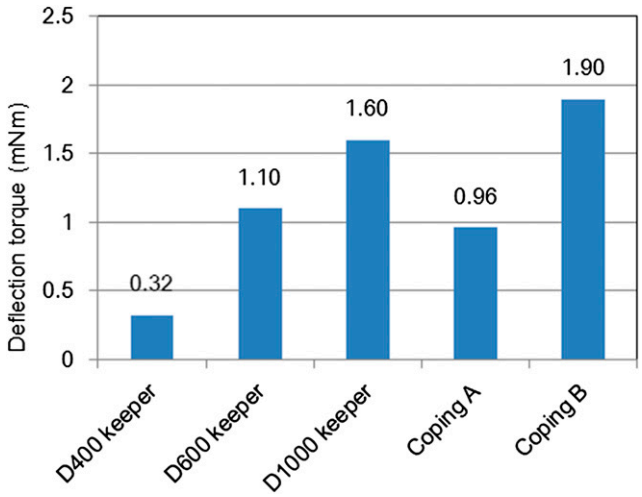

Figure 5 Magnetically induced torques of the tested devices.

devices to a dental prosthesis or abutment teeth should be checked before and after MRI because of the possibility of cement degradation.

The deflection force of Coping B, which was composed of cast magnetic alloy, showed a deflection force approximately eight times greater than that of a more commonly used keeper (Coping A). The deflection force is dependent on the strength of the static magnetic field, maximum spatial gradient and object characteristics, including mass and magnetic susceptibility.[6,11,12] Large ferromagnetic prostheses (*e.g.* a bar attachment) would thus carry a higher risk of migration during MRI. Therefore, large prostheses made of ferromagnetic material should be removed before MRI.

The torque acting to align the long axis of an object with the magnetic field is produced by the static field in an MR system.[4,18,30] According to the ASTM F2213 standard for magnetically induced torque, torque is evaluated using a torsional pendulum method, where the specimen is placed on a platform at the centre of the MR system where the magnetic field is uniform, and torque is determined from measurement of the holder's deflection angle from its equilibrium position. However, there are some difficulties adapting this standard to keepers. One of the difficulties is that the apparatus is large; however, the measurement area at the centre of the MR system is quite limited.

Another difficulty is the reproducibility of measurements of the torsional spring in the testing jig as recommended in the ASTM standard because the torsional spring diameter should be chosen for each specimen to change the spring constant, and the torque is determined by calculating the rotation angle and spring constant. However, its platform is supported by fixed upper and lower torsional springs; therefore, it is not possible to change or adjust the spring strength for each specimen; moreover, the spring is included in the platform, so there is a possibility that the theoretically calculated torque from the spring constant will differ from the actual torque.

Yet another difficulty is measurement interactions from the magnetic field from not only torque but also magnetically induced forces produced in specimens in the static field of an MR system. Theoretically, the field gradients are uniform at the centre of the magnet bore, and the deflection force is not strong enough to measure the torque; however, a keeper in which a ferromagnetic substance becomes magnetized and behaves like a magnet, then, the magnetic field is highly disturbed near the keeper.[10,17,18,20,32,33] Accordingly, the keeper is influenced by loads that are unbalanced or offset from a non-uniform field. These forces are proportional to magnetic field strength; therefore, especially in a high-field-strength MR system, translational movement force in a ferromagnetic specimen cannot be neglected in the measurement of torque.[32,33]

Therefore, we designed a simple and reproducible method to measure the torque of ferromagnetic materials in a low-field-strength MR system.

By using a torque angle indicator, we produced measurements easily, with good reproducibility and great accuracy. The resultant torque in a GIGAUSS D1000, which is one of the largest commercially available keepers, in a 0.3-T MR system was 1.60 mN m and that of Coping B made of cast magnetic alloy was 1.90 mN m. Torque is proportional to the static magnetic field strength;[18,32] therefore, the torques generated in Copings A and B during 3.0-T MRI are expected to be 16.0 and 19.0 mN m, respectively. The values are sufficiently smaller than the torques applied to dental implant abutment screws. Several manufacturers recommend closing torque values for implant screws $>20\ \mathrm{N\,cm^{-1}}$ (for example, Steri-Oss™ recommends $35\ \mathrm{N\,cm^{-1}}$ and Sulzer Calcitek recommends $28\ \mathrm{N\,cm^{-1}}$).[34]

In conclusion, the results of this experiment conducted according to the ASTM F2182-09 standard testing method are applicable to other MR sequences to estimate RF-induced heating from the SAR. The relatively mild RF-induced heating of magnetic dental attachments during 3-T MRI should not pose a risk to patients. While their magnetically induced torques were small enough, their magnetically induced deflection forces tended to exceed the acceptable limit.

Ideally, ferromagnetic keepers are removed from the oral area before MRI; however, it is not always in the best interest of the patient. From a safety perspective, the fixation of such devices should be inspected before and after MRI.

References

1. Shellock FG, Spinazzi A. MRI safety update 2008: part 2, screening patients for MRI. *AJR Am J Roentgenol* 2008; **191**: 1140–9. doi: 10.2214/AJR.08.1038.2
2. Shellock FG, Valencerina S. Septal repair implants: evaluation of magnetic resonance imaging safety at 3 T. *Magn Reson Imaging* 2005; **23**: 1021–5. doi: 10.1016/j.mri.2005.10.010
3. Muranaka H, Horiguchi T, Usui S, Ueda Y, Nakamura O, Ikeda F. Dependence of RF heating on SAR and implant position in a 1.5T MR system. *Magn Reson Med Sci* 2007; **6**: 199–209. doi: 10.2463/mrms.6.199
4. Walsh EG, Brott BC, Johnson VY, Venugopalan R, Anayiotos A. Assessment of passive cardiovascular implant devices for MRI compatibility. *Technol Health Care* 2008; **16**: 233–45.
5. Willinek WA, Schild HH. Clinical advantages of 3.0 T MRI over 1.5 T. *Eur J Radiol* 2008; **65**: 2–14. doi: 10.1016/j.ejrad.2007.11.006
6. Shellock FG, Valencerina S. *In vitro* evaluation of MR imaging issues at 3T for aneurysm clips made from MP35N: findings and information applied to 155 additional aneurysm clips. *ANJR Am J Neuroradiol* 2010; **31**: 615–19. doi: 10.3174/ajnr.A1918
7. Kuhl CK, Träber F, Schild HH. Whole-body high-field-strength (3.0-T) MR imaging in clinical practice. Part I. Technical considerations and clinical applications. *Radiology* 2008; **246**: 675–96. doi: 10.1148/radiol.2463060881
8. Hasegawa M, Umekawa Y, Nagai E, Ishigami T. Retentive force and magnetic flux leakage of magnetic attachment in various keeper and magnetic assembly combinations. *J Prosthet Dent* 2011; **105**: 266–71. doi: 10.1016/S0022-3913(11)60042-5
9. ASTM Standard F2182-09. *Standard test method for measurement of radio frequency induced heating on or near passive implants during magnetic resonance imaging*. West Conshohocken, PA: ASTM International; 2009.
10. ASTM Standard F2052. *Standard test method for measurement of magnetically induced displacement force on medical devices in the magnetic resonance environment*. West Conshohocken, PA: ASTM International; 2006.
11. Kemper J, Priest AN, Schulze D, Kahl-Nieke B, Adam G, Klocke A. Orthodontic springs and auxiliary appliances: assessment of magnetic field interactions associated with 1.5 T and 3 T magnetic resonance systems. *Eur Radiol* 2007; **17**: 533–40. doi: 10.1007/s00330-006-0335-x
12. New PF, Rosen BR, Brady TJ, Buonanno FS, Kistler JP, Burt CT, et al. Potential hazards and artifacts of ferromagnetic and nonferromagnetic surgical and dental materials and devices in nuclear magnetic resonance imaging. *Radiology* 1983; **147**: 139–48. doi: 10.1148/radiology.147.1.6828719
13. Gonda T, Maeda Y. Why are magnetic attachments popular in Japan and other Asian countries? *Jpn Dent Sci Rev* 2011; **47**: 124–30. doi: 10.1016/j.jdsr.2011.04.004
14. Gillings BR. Magnetic retention for overdentures. Part II. *J Prosthet Dent* 1983; **49**: 607–18. doi: 10.1016/0022-3913(83)90382-7
15. Gillings BR. Magnetic retention for complete and partial overdentures. Part I. *J Prosthet Dent* 1981; **45**: 484–91. doi: 10.1016/0022-3913(81)90032-9
16. Gonda T, Ikebe K, Ono T, Nokubi T. Effect of magnetic attachment with stress breaker on lateral stress to abutment tooth under overdenture. *J Oral Rehabil* 2004; **31**: 1001–6. doi: 10.1111/j.1365-2842.2004.01324.x
17. Miyata K, Hasegawa M, Abe Y, Tabuchi T, Namiki T, Ishigami T. Radiofrequency heating and magnetically induced displacement of dental magnetic attachments during 3.0 T MRI. *Dentomaxillofac Radiol* 2012; **41**: 668–74. doi: 10.1259/dmfr/17778370
18. ASTM Standard F2213-06. *Standard test method for measurement of magnetically induced torque on medical devices in the magnetic resonance environment*. West Conshohocken, PA: ASTM International; 2011.
19. ASTM Standard F2182-02a. *Standard test method for measurement of radio frequency induced heating near passive implants during magnetic resonance imaging*. West Conshohocken, PA: ASTM International; 2002.
20. Hasegawa M, Miyata K, Abe Y, Ishigami T. Radiofrequency heating of metallic dental devices during 3.0 T MRI. *Dentomaxillofac Radiol* 2013; **42**: 20120234. doi: 10.1259/dmfr.20120234
21. Amjad A, Kamondetdacha R, Kildishev AV, Park SM, Nyenhuis JA. Power deposition inside a phantom for testing of MRI heating. *IEEE Trans Magn* 2005; **41**: 4185–7. doi: 10.1109/tmag.2005.854840
22. Nordbeck P, Fidler F, Weiss I, Warmuth M, Friedrich MT, Ehses P, et al. Spatial distribution of RF-induced E-fields and implant heating in MRI. *Magn Reson Med* 2008; **60**: 312–19. doi: 10.1002/mrm.21475
23. Baker KB, Tkach JA, Nyenhuis JA, Phillips M, Shellock FG, Gonzalez-Martinez J, et al. Evaluation of specific absorption rate as a dosimeter of MRI-related implant heating. *J Magn Reson Imaging* 2004; **20**: 315–20. doi: 10.1002/jmri.20103
24. Baker KB, Tkach JA, Phillips MD, Rezai AR. Variability in RF-induced heating of a deep brain stimulation implant across MR systems. *J Magn Reson Imaging* 2006; **24**: 1236–42. doi: 10.1002/jmri.20769
25. Pigg M, Baad-Hansen L, Svensson P, Drangsholt M, List T. Reliability of intraoral quantitative sensory testing (QST). *Pain* 2010; **148**: 220–6. doi: 10.1016/j.pain.2009.10.024
26. List T, Leijon G, Svensson P. Somatosensory abnormalities in atypical odontalgia: a case-control study. *Pain* 2008; **139**: 333–41. doi: 10.1016/j.pain.2008.05.002
27. Green BG. Heat pain thresholds in the oral-facial region. *Percept Psychophys* 1985; **38**: 110–14. doi: 10.3758/bf03198847
28. Ramsköld LO, Fong CD, Strömberg T. Thermal effects and antibacterial properties of energy levels required to sterilize stained root canals with an Nd:YAG laser. *J Endod* 1997; **23**: 96–100. doi: 10.1016/s0099-2399(97)80253-1
29. Gutknecht N, Franzen R, Meister J, Vanweersch L, Mir M. Temperature evolution on human teeth root surface after diode laser assisted endodontic treatment. *Lasers Med Sci* 2005; **20**: 99–103. doi: 10.1007/s10103-005-0347-9
30. Shellock FG, Shellock VJ. Metallic stents: evaluation of MR imaging safety. *AJR Am J Roentgenol* 1999; **173**: 543–7. doi: 10.2214/ajr.173.3.10470877
31. Abe Y, Hasegawa M, Uchida T, Kiuchi M. Dental cement strength for luting to a magnetic keeper of keeper-bonding technique. [In Japanese.] *J J Mag Dent* 2011; **20**: 37–43.
32. Luechinger R, Duru F, Scheidegger MB, Boesiger P, Candinas R. Force and torque effects of a 1.5-Tesla MRI scanner on cardiac pacemakers and ICDs. *Pacing Clin Electrophysiol* 2001; **24**: 199–205. doi: 10.1046/j.1460-9592.2001.00199.x
33. Sasaki Y, Akutagawa M, Emoto T, Tegawa Y, Kinouchi Y. Theoretical study of evaluation method for MRI metal artifact. *Conf Proc IEEE Eng Med Biol Soc* 2013; **2013**: 1073–6. doi: 10.1109/EMBC.2013.6609690
34. Weiss EI, Kozak D, Gross MD. Effect of repeated closures on opening torque values in seven abutment-implant systems. *J Prosthet Dent* 2000; **84**: 194–9. doi: 10.1067/mpr.2000.108069